Journal of Pharmaceutical Sciences 114 (2025) 103822

Contents lists available at ScienceDirect

Journal of Pharmaceutical Sciences

journal homepage: www.elsevier.com/locate/xphs

Pharmaceutics, Drug Delivery and Pharmaceutical Technology

Ex vivo-in vitro protein adsorption and *in vivo* anti-inflammatory effects of zwitterionized PVA hydrogel implants in the New Zealand albino rabbit eye

Onyinye Jennifer Uwaezuoke, Lisa Claire du Toit, Pradeep Kumar, Naseer Ally, Yahya Essop Choonara *

Wits Advanced Drug Delivery Platform, School of Therapeutic Sciences, Faculty of Health Sciences, University of the Witwatersrand, 7 York Road, Parktown, Johannesburg, 2193, South Africa

ARTICLE INFO

Editor: Dr K Audus

Keywords:
Hydrogel
Ocular devices
Protein resistance
Zwitterionization
Inflammation

ABSTRACT

Implantable ocular devices are increasingly used to overcome the drug delivery challenges presented by the physio-anatomical barriers of the eye. Protein adsorption onto the biomaterial occurs within minutes of implantation and is usually the first step in the fouling process that could culminate in implant/device failure, infection, or even death if the infection is not properly managed. The eye can easily be damaged by any inflammatory process due to its immune privilege status, hence, the need for biomaterials that would inherently limit protein adsorption and reduce inflammation. Herein, a super hydrophilic hydrogel ocular device was formulated via facile photo-initiated crosslinking polymerization between polyvinyl alcohol and sulfobetaine methacrylate, 2 polymers that have previously been employed individually, for surface modification of biomaterials towards protein resistance. Protein adsorption onto the hydrogel was studied *in vitro* and *ex vivo* using a complex protein solution, and rabbit aqueous and vitreous humour, respectively. *In vivo* ocular cytocompatibility was studied in New Zealand albino rabbits by subconjunctival implantation over a period of 8 weeks. The concentration of the zwitterionic monomer significantly affected protein adsorption *in vitro*, and impacted the foreign body response *in vivo*. *In vivo* results after 1 week showed a graded acute inflammatory response indicative of tissue repair that resulted in full integration by the 8th week.

Abbreviations

AH	aqueous humour
VH	vitreous humour
ATF	artificial tear fluid
PVA	Polyvinyl alcohol
PVAGMA	Polyvinylalcohol glycidyl methacrylate
DED	Dry eye disease
SBMA	Sulfobetaine Methacrylate
SDS	Sodium dodecyl sulphate
WRAF	Wits Research animal facility
MNGBC	Multi-nucleated foreign body giant cells

Introduction

The search for successful materials for various applications in ocular drug delivery is a continuing effort in the drive to overcome the challenges associated with this site of delivery. These challenges include tissue reaction to implanted biomaterials and invasiveness at anterior and posterior target locations. Incidentally, though certain ocular tissues such as the retina are known to be immune-privileged sites, inflammatory response to implanted devices remain a challenge,[1] which is further complicated by the diverse nature of ocular tissues existing in close proximity to each other. Ocular implants such as intraocular lenses, contact lenses, and punctal plugs still suffer from major challenges such as protein adsorption and the consequent fouling and biofilm formation.[1] Biofilm formation is a major concern for implantable ocular devices often leading to infections and sight threatening inflammatory processes such as keratitis. Due to the proximity of various ocular tissues, inflammation in one section of the eye results in adverse effects in sites distant from the site of inflammation. Innomata and colleagues, while highlighting that devices such as contact lenses constitute a specific risk factor for dry eye disease (DED), also posited that scarcity of treatment strategies that target specific factors may threaten the success

* Corresponding author at: Division of Ophthalmology, Department of Neurosciences, Faculty of Health Sciences, University of the Witwatersrand, 7 York Road, Parktown, Johannesburg, 2193, South Africa.
E-mail address: Yahya.choonara@wits.ac.za (Y.E. Choonara).

https://doi.org/10.1016/j.xphs.2025.103822
Received 4 October 2024; Received in revised form 6 May 2025; Accepted 6 May 2025
Available online 8 May 2025

of current treatment strategies.[2]

Targeted biomaterial design may be a treatment strategy that addresses specific factors in DED caused by contact lens wear. In addition, other devices such as punctal plugs designed for the treatment of DED can intrinsically result in inflammation that further exacerbates existing DED.[3] Likewise, scleral lenses used in the treatment of inflammatory ocular surface conditions need to be designed in a manner that elicits minimal reaction from ocular tissues in order to prevent the exacerbation of an already inflamed surface.[4] The design, form, size, structure, components, rigidity, hydrophobicity, and, more importantly, tissue implantation site of ocular devices have all been shown to contribute to the type and extent of protein adsorption on any implanted biomaterial and these in turn determine the phenotype of macrophages that will mediate the inflammatory response.[5] Xu and colleagues, in their study, established that hydrophobicity was a key factor in determining the extent of the inflammatory response.[6] Ishihara and coworkers highlighted the additional influence of hydrogel porosity on increased protein adhesion, as observed in their study. They recorded a higher level of protein adsorption on their more hydrophilically-modified hydrogel and attributed it to the diffusion of the small molecular weight lysozyme into the gels.[7] As their hydrogel was surface modified, this observation may also bring to the fore the importance of bulk modification when compared to surface modification. Although several researchers have studied the nature of inflammatory response to implanted biomaterials, the majority of these studies for ocular biomaterials were studied at sites other than the eye.[8]

Hydrogels occupy an important niche both for drug delivery and other ocular applications due to their distinct properties such as biocompatibility, close resemblance to extracellular matrix, ease of fabrication, and versatility in terms of application and manoeuvrability.[9] Hydrogels are prepared from synthetic, semi-synthetic or natural polymers which are either physically or chemically crosslinked to provide a 3-dimensional porous network enclosing a high volume of water. They have been studied for local, targeted, controlled, and smart drug delivery systems[10] as contact lens, punctal plugs and other applications. In ocular drug delivery, hydrogels are increasingly being used as a platform to overcome specific challenges to drug delivery for both the anterior and posterior segments of the eye. In this work, zwitterionization of a methacrylated polyvinyl alcohol (PM) polymer using sulfobetaine methacrylate (SM) in a facile photoinitiated crosslinking polymerization process was undertaken for the fabrication of an ocular hydrogel device. Various characteristics of the hydrogel, including its mechanical strength, low biofouling and cell adhesion potential, ocular cell cytotoxicity, superhydrophilicity, and transparency had previously been established in an earlier study.[11] In this investigation, the SM content was varied to enable the evaluation of its effect on protein adsorption *in vitro* and *ex vivo* and ultimately on inflammation when implanted *in vivo* in New Zealand albino rabbits' eye.

Materials and methods

Materials

Sulfobetaine methacrylate monomer, and polyvinyl alcohol methacrylate were synthesized as previously reported[12,13] while polyvinyl alcohol methacrylate-co-sulfobetaine methacrylate was synthesized for the first time via photoinitiated crosslinking polymerization.[11] Micro BCA™ Protein Assay Kit (Thermo Fischer Massachusetts, USA), chicken egg lysozyme, mucin, and bovine serum albumin (Sigma Aldrich, Germany). Irgacure 2959, Polyethylene glycol dimethacrylate (Mn 750) were purchased from Sigma (Sigma-Aldrich, St Louis, MO, USA).

Preparation of hydrogels

Zwitterionization was modulated by varying the percentage content of SBMA in the hydrogels. Hydrogel samples prepared with 0%, 20% and 33% w/w SBMA were assessed via *in vitro*, and *ex vivo* protein adsorption studies. They were also subjected to *in vivo* cytocompatibility analysis to evaluate the potential effect of zwitterionization on the hydrogels. Codes were assigned to identify samples according to the content of the 2 polymers used as indicated in Table 1. PM and SM coded for polyvinyl alcohol methacrylate and sulfobetaine methacrylate, respectively, while the numbers that followed each name indicated the weight percentage of each respective polymer in the sample.

In vitro quantitative determination of protein adsorption onto hydrogel discs

The BCA micro assay kit was employed in the determination of the quantity of protein adsorbed onto the hydrogel *in vitro* from a complex protein solution consisting of mucin (0.5 mg/mL), lysozyme (1.2 mg/mL), bovine serum albumin (3.88 mg/mL), and $CaCl_2$ (2 mg), in 100 mL phosphate buffered saline (PBS). The constituent proteins of the artificial protein solution employed represent the dominant proteins in rabbit tear fluid (lysozyme, albumin, mucin),[14] and is of a similar composition to that employed in other investigations characterizing protein absorption on ocular hydrogels.[15] Some of these proteins also have a notable presence in the aqueous humor (AH) (albumin),[16] and the vitreous humour (VH) (albumin).[17] Thus, an *in vitro* model was prepared to identify the interactions of the hydrogel with a fluid containing the dominant proteins present in the ocular fluids of rabbits.[15] Briefly, 4 mm discs were punched from the hydrogel samples and equilibrated in artificial tear fluid (ATF). These were subsequently immersed in 5 mL protein solution, placed in an orbital shaker set at 37°C and 40 rpm for 1.5 hours. The discs were retrieved thereafter and rinsed three times with PBS. Sodium dodecyl sulphate (1 % $^{w}/_{v}$, 2 mL) was used to detach the protein adsorbed on the hydrogels by incubating at 37°C for 1 hour. The calibration curve was constructed using the complex protein solution in which the discs were subsequently immersed. Quantitation was undertaken by reading off the concentration on an Implen NanoPhotometer® (Implen GmbH, Munchen Germany) using the BCA assay tool.

Ex vivo qualitative determination of protein adsorption onto hydrogel discs

Discs from both the zwitterionized and unzwitterionized hydrogels were formed with a 6 mm biopsy punch. These were incubated in 1 mL aqueous and vitreous humour samples, obtained from New Zealand albino rabbits, at 37°C for 90 minutes in an orbital shaker. Subsequently, the discs were washed 3 times with PBS at pH 7.4. The adsorbed protein on the discs were thereafter extracted with a 1% $^{w}/_{v}$ sodium dodecyl sulphate (SDS) solution. A modified form of the sodium dodecyl sulfate polyacrylamide gel electrophoresis (SDS-PAGE) was used to elucidate the pattern of adsorbed proteins on the hydrogel samples as it provides information regarding the molecular size along with intermolecular disulfide bonds of proteins.[15] The extract from the 1 % w/v SDS solution was mixed with about 100 μL electrophoresis sample buffer (1 mM EDTA, 10 mM Tris-HCl, pH 8.0, 2.5 % SDS and 5 % β mercaptoethanol) and boiled for 15 minutes and thereafter centrifuged at 9000 rpm for 10 minutes to extract the adsorbed proteins. The supernatant (10 μL) was applied to a 10 % gradient electrophoresis gel and electrophoresis conducted using MINI-PROTEAN® 3 cell (Bio-Rad, USA) at 200 V. The separated protein bands were visualized by staining the gels with about 1 % w/v Coomassie brilliant blue in a 40% methanol/10% acetic acid solution for 1 hour and subsequently destained in a solution containing

Table 1
Codes and polymer content for sample hydrogels.

Component Codes	PM100-SM0	PM80-SM20	PM67-SM33
Polyvinyl alcohol methacrylate (PM)	100%	80%	67%
Sulfobetaine methacrylate (SM)	0%	20%	33%

40% methanol and 10% glacial acetic acid.

In vivo assessment of cytocompatibility of the hydrogel discs

Ethics clearance (certificate no 2021-07-03C) for the *in vivo* implantation study in New Zealand albino rabbits was obtained from the Animal Research Ethics Committee of the University of Witwatersrand, Johannesburg, South Africa. A total of 15 male and female rabbits weighing between 2.5 to 3.5 kg were received at the Wits Research Animal Facility (WRAF) a week prior to the commencement of the study and acclimatized for 5 days. The animals were housed individually at the WRAF, maintained at a temperature of 25 °C ± 2 °C and humidity 55 % ± 5 % with a 12-hour light/night cycle and having free access to standard animal food and water. Following a previously established protocol with modification, 4 mm x 0.75 mm hydrogel discs were punched and sterilized and implanted into the sub conjunctival space of the rabbits' right eye (while the left eye served as a control) by an ophthalmologist following aseptic techniques.[18,19] Prior to the procedure, the rabbits were anesthetized with an intraperitoneal injection of a mixture of ketamine (65 mg/Kg) and xylazine (7.5 mg/kg). At 1, 4, and 8 weeks respectively, 5 rabbits were euthanized with an overdose of phenobarbital sodium, and the hydrogel discs explanted. These were fixed in 10 % w/v neutral buffered saline and afterwards, samples were prepared for scanning electron microscopic (SEM) viewing using a modified version of a previously applied protocol.[20] Briefly, a representative explanted disc was dehydrated in a serially concentrated alcohol maintained for 15 minutes at each concentration (50 %, 60 %, 70 %, 80 %, 90 %, and 100 % $^{v}/_{v}$), air dried, sputter coated with gold/palladium, and examined under the SEM. The SEM images of the implanted discs were compared with that of hydrogel discs that were not implanted. Sections of representative explanted discs were also stained with hematoxylin-eosin and photographs were acquired. Histopathological examination of the capsular tissue surrounding the implanted disc was also undertaken.

Results

In vitro and ex vivo protein adsorption

The results of *in vitro* protein adsorption obtained using the BCA assay are displayed in Fig. 1. The level of *in vitro* protein adsorption from across all samples was low with the highest amount of protein (0.1036 ± 0.4224 μg/mm^2) being adsorbed by PM100-SM0 hydrogel. There was a gradual decrease in the level of adsorbed protein as the concentration of modifying monomer, SBMA, in the hydrogel increased. Statistical analysis showed that the addition of SBMA contributed significantly to protein resistance *in vitro* ($p = 0.000531$). The hydrogel with the highest level of SBMA had the least adsorbed protein (0.0487 ± 0.263 μg/mm^2) *in vitro*.

In Fig. 2, the *ex vivo* protein adsorption obtained from the aqueous and vitreous humour collected from rabbits is displayed. The non-zwitterionized hydrogel, PM100-SM0, that had the highest adsorption from *in vitro* protein mixture had the least adsorption in both aqueous and vitreous humour studies. The amount of protein adsorbed from the

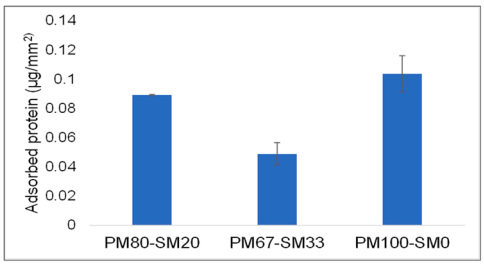

Fig. 1. Protein adsorption on hydrogel discs with differing SBMA content.

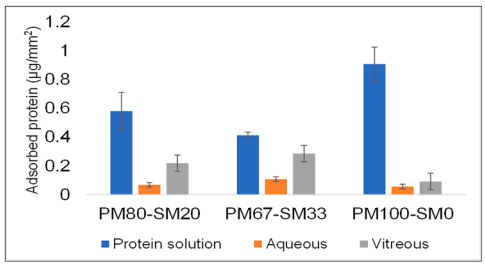

Fig. 2. *Ex vivo* protein adsorption in aqueous and vitreous humour.

aqueous was notably lower than that from the vitreous humour samples, but not significantly ($p = 0.0678$). In addition, the total amount of protein adsorbed per unit area of the hydrogel discs were notably lower than that adsorbed from the artificial protein mixture *in vitro* ($p = 0.01284$ for AH and $p = 0.02286$ for VH).

Qualitative determination of adsorbed protein by SDS-PAGE

Fig. 3 depicts the digital image of a representative run on SDS-PAGE for the qualitative assessment of the protein adsorbed on hydrogel discs from *in vitro* assessment. The 2 lanes at the opposite ends of the gel represent the protein stock solution (containing a mixture of the proteins used) and the protein marker, respectively. Each constituent protein sample was placed in 2 wells. One protein band was visible from all the wells containing extracts from the hydrogel and was most likely responsible for measured adsorption on the gels. An alternative explanation may be that the level of the other proteins adsorbed on the hydrogel were extremely low and hence could not be resolved by the 10 % acrylamide gel gradient as that the limit of detection by SDS-PAGE stained with Coomassie blue is 100 ng. Protein concentration of the sample using salting out techniques could resolve this. In a similar manner, proteins adsorbed from the aqueous and vitreous humour during *ex vivo* experiments were also subjected to analysis by electrophoresis. Fig. 4 shows the results of electrophoresis for determination of protein adsorption from aqueous and vitreous humour samples. The results were similar to that obtained from *in vitro* protein adsorption analysis and shows only the protein marker lane is visible.

In vivo evaluation of hydrogel discs in New Zealand albino rabbits

Fig. 5 shows a representative image of the rabbit eye directly after hydrogel disc implantation, while images in Fig. 6 were captured after 8 weeks of implantation and show the integration of the hydrogel disc into the superior bulbar conjunctiva.

To determine whether the *in vivo* inflammatory response is dependent on the SBMA content, hydrogel discs containing different levels of SBMA, PM67-SM33 and PM80-SM20, were implanted for the 1-week study. The explanted hydrogel disc had no visible signs of

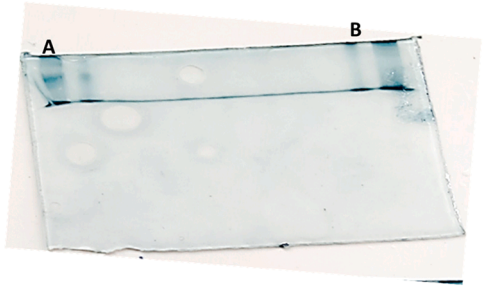

Fig. 3. SDS-PAGE of proteins adsorbed on hydrogels from *in vitro* analysis. A represents the lane for the protein marker and B represents the lane for the protein stock solution.

Fig. 4. SDS-PAGE of protein from *ex vivo* studies showing the single lane (A) for the protein marker.

Fig. 5. Representative image of a rabbit eye directly after implantation.

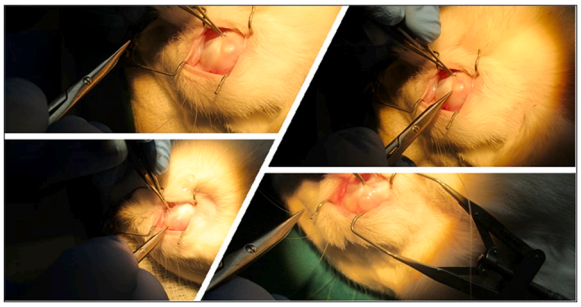

Fig. 6. Digital image of PM67-SM33 hydrogel disc 8 weeks post-implantation.

desquamation nor were there any adhering tissues as can be seen from Fig. 7. Similarly, the hydrogel observed embedded in the tissue in the histological images did not have cells adhering to it. In Fig. 8, the histological images of sections from the tissues surrounding the implant after a week are displayed. The arrows in Fig. 8 (C and I) point to fragments of the implant found embedded in tissue sections for PM67-SM33 and PM80-SM20 respectively. No cells can be seen on these implant fragments embedded in the tissues from these images. Histological reports graded the presence of different cellular components of inflammation observed in the tissue samples. These are summarized in

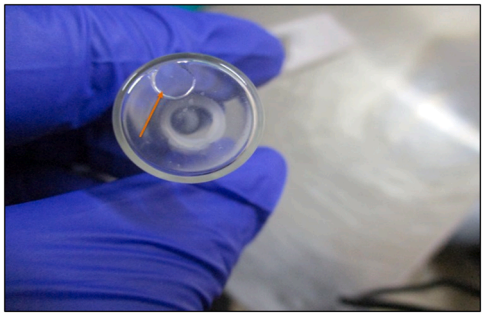

Fig. 7. Digital image of a hydrogel disc explanted after 8 weeks.

Table 2. Histological images of tissues obtained from area surrounding the hydrogel discs explanted from rabbit's subconjunctival space after 4 weeks, and 8 weeks are shown in Figs. 9 and 10, respectively.

The types and number of cells identified histologically in the tissue sections from the immediate vicinity of the implanted were shown in Table 2 and in Figs. 8, 9, and 10, the images from tissue sections obtained from the tissues surrounding hydrogels at the end of week 1, week 4, and week 8 are displayed. These included heterophils, lymphoplasmacytic cells, macrophages, and multinucleated giant body cells. Multinucleated giant body cells (MNGBC), for instance, were graded (+2) in the immediate tissues surrounding the cavity created by the procedure. MNGBC are usually formed by the fusion of macrophages activated in the acute phase when their attempt at phagocytosis fails particularly because of the size of the presenting stimuli. The response to the implant after a week majorly represented an acute phase of tissue repair and encapsulation of the foreign material. In hydrogel PM67-SM33, the stromal response accompanied by more mature collagen fibres with horizontally arranged layers, represents an advanced level of tissue repair occurring after a week. The number of multinucleated foreign body giant cells (MNGBC) were also lower in PM67-SM33, and this correlates with the *in vitro* protein adsorption study findings. Histological reports showed that there was minimal presence of inflammatory cells by the 4th week and involved heterophils, macrophages, lymphoplasmacytic cells and a few MNGBC. These were associated with one sample that contained a hair shaft as a foreign material in the cystic space. All other samples showed normal mucosa and submucosa with cystic spaces lined or encircled by layers of plump fibroblasts interspersed with connective tissues and forming granulation tissue in some samples.

There was minimal capsule formation as can be observed in the histological images in Fig. 9. One of the hydrogel discs was not found in one of the rabbits by the end of the 1st and 4th week. By the 8th week, histological analysis indicated the formation of cystic encapsulation with a fibrosis layer measuring from 4 cells thickness to a thickness of 0.1μm in one sample. Fig. 11A shows the size of the collagen capsules formed around the implant at various time points after explantation. These measurements were obtained employing the Image J yellow measuring tool shown in Fig. 11B. The inflammatory response to implanted biomaterials usually presents as a fibrotic collagen capsule that forms around the implanted device, and may be evaluated through its size and nature.[21]

Fig. 11 shows that this capsule was absent at 1 week but present by the 4th and 8th week. There was no significant difference ($p > 0.05$) between the sizes of the collagen capsules at both time periods. In addition, in most of the sections captured by histology, this capsule was identified as a layer of fibroblasts intermingled with synthesized collagen and connective tissues. This represents the formation of new tissues through which connection with the local tissue environment may be maintained, a very welcome development.

The morphology of cells attached to the explanted hydrogel discs was additionally studied via Scanning Electron Microscopy, SEM. Fig. 12 (A3 and A4) shows the SEM image of a representative PM67-SM33 hydrogel disc explanted after 4 weeks while Fig. 12 (A1 and A2) are SEM images of a control hydrogel disc that was not implanted. Cells identified on the SEM images of explanted hydrogel were minimal and occupied less than 50 % of the disc view captured under the SEM as can be visualized from Fig. 12 (A3 and A4). These represent lymphocytes, heterophils, and macrophages. Fig. 13 depicts representative SEM images of the same hydrogel explanted after 8 weeks. The morphology of the cells slightly differs from the images in Fig. 12 (A3 and A4).

The presence of inflammatory cells was limited to the presence of a few single cell lymphocytes, heterophils and plasma cells. On one of the implants shown in Fig. 13, lymphocytes and macrophages fusing to form multinucleated giant body cells were identified. Multinucleate giant body cells were associated with the presence of a foreign material embedded adjacent to the cystic space left by the implant.

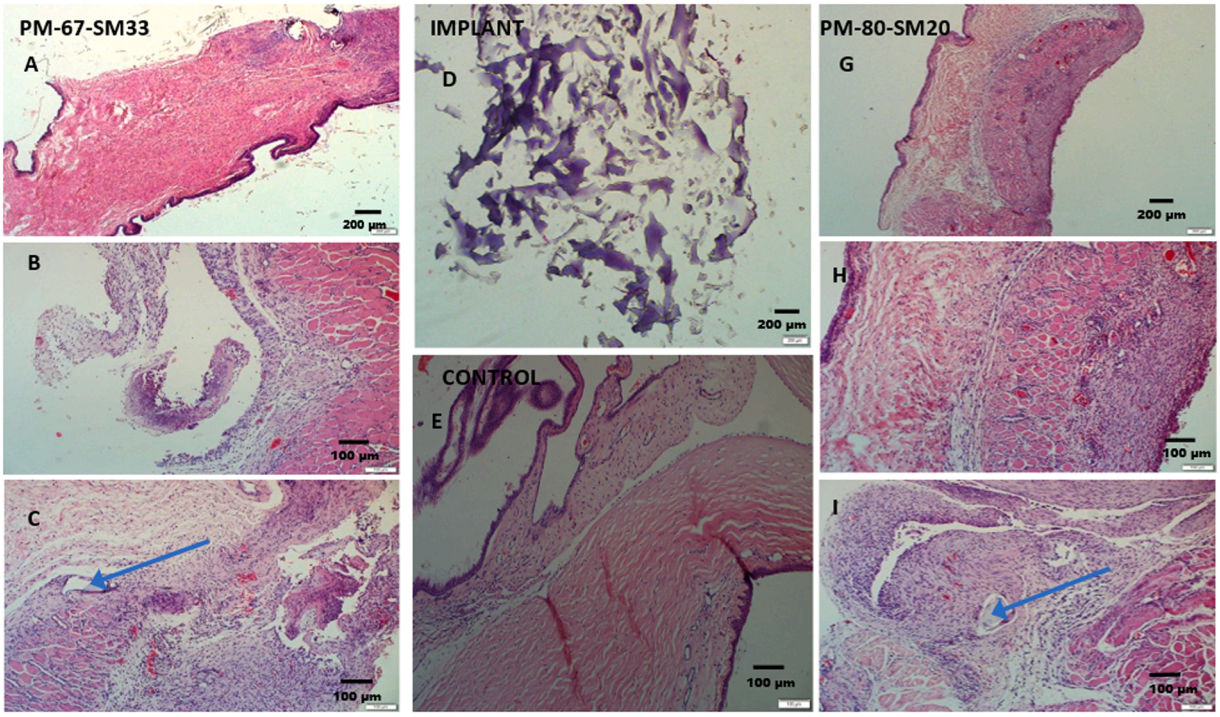

Fig. 8. Histopathological images depicting the effect of implanted hydrogels PM67-SM33 (A, B, C) and PM80-SM20 (F, G, H) on conjunctival tissues after 1 week. D and E are sections of the explanted hydrogel and the control eye respectively. The blue arrows show the implant embedded in the tissue.

Table 2
Cell types appearing in each subsection of the tissue.

Section	PM80-SM20		PM67-SM33	
Inner layer	+2 epithelioid macrophages	Heterophils	+2 epithelioid macrophages	Single heterophil
Surrounding stroma	3+ thickness	Lymphoplasmacytic cell 1+	Rich fibrous collagen	
MNGBC*	3.5+		1+	

Discussion

The results of the *in vitro* protein adsorption study observation is in congruence with other studies; however, the level of protein adsorbed in the current study is below that previously reported.[22-24] It is pertinent to note that the protein constitution of the artificial protein solution used in different studies as well as the evaluation method varied and may have contributed to observed differences in the total adsorbed protein observed for individual studies. In this report, the protein solution used represents a complex protein solution constituted from 3 different proteins commonly found in tear fluid; lysozyme, albumin, and mucin[23,25]

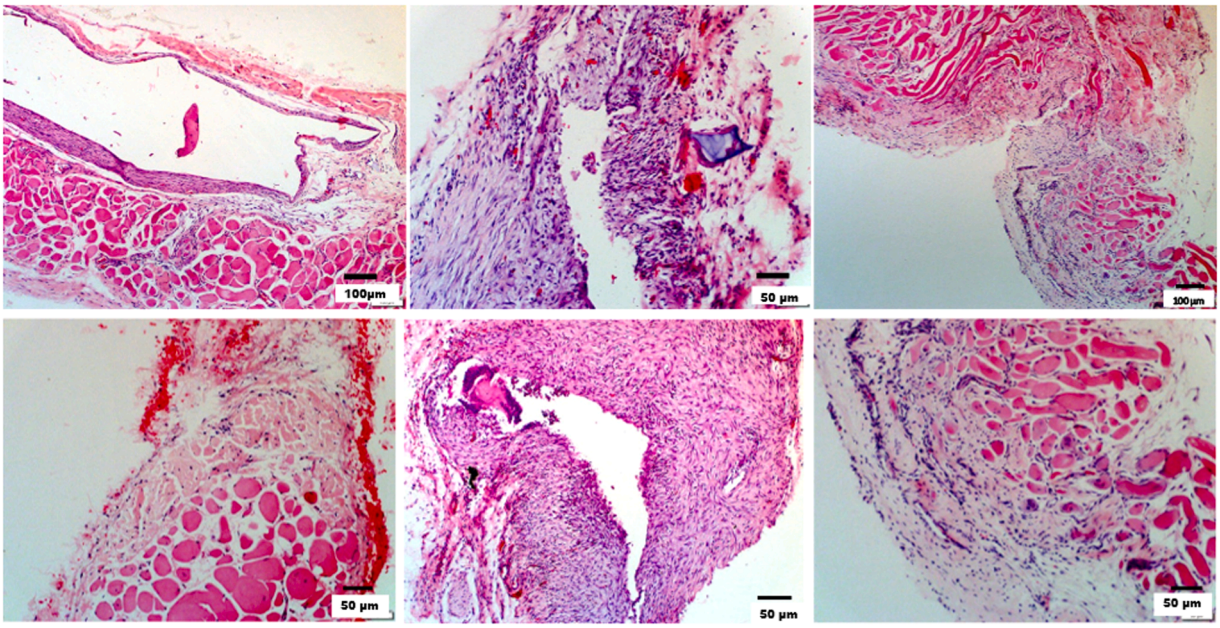

Fig. 9. Histopathological images of different sections depicting the effect of implanted hydrogel PM67-SM33 discs on conjunctival tissues after 4 weeks.

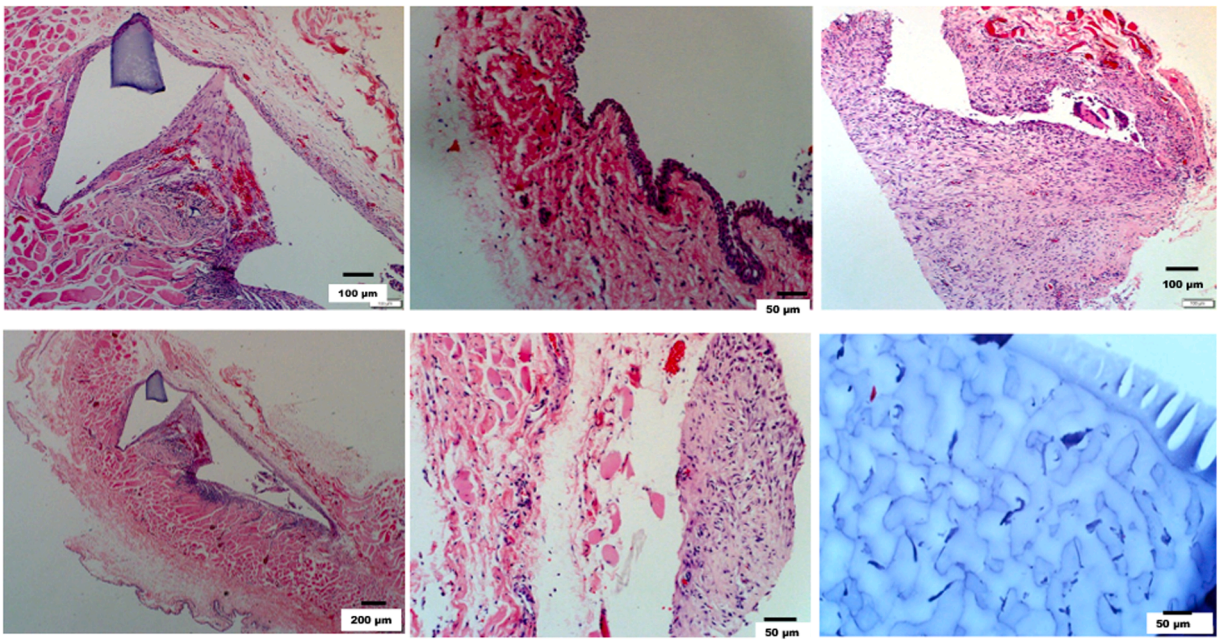

Fig. 10. Histopathological images depicting the effect of implanted hydrogel PM67-SM33 discs on conjunctival tissues after 8 weeks. The blue slide is the explanted hydrogel implant.

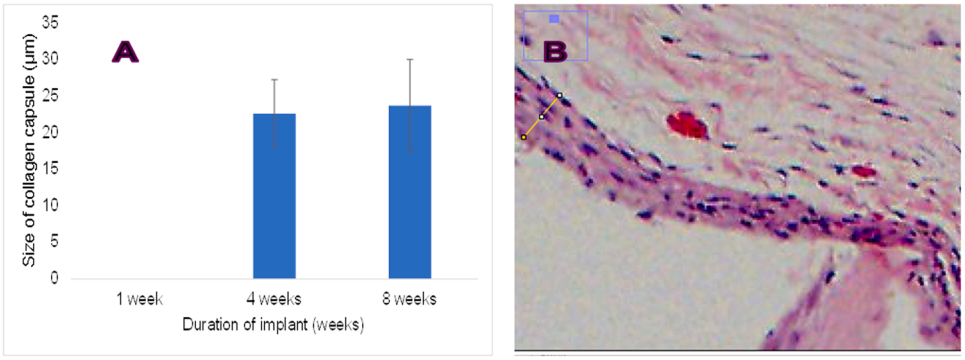

Fig. 11. Size of collagen capsule formed around the implant after 1-, 4-, and 8-weeks implantation (A). Example image depicting measurement with Fiji Image J yellow tool (B).

(albumin also being a dominant protein present in the AH and VH). In addition, during protein evaluation, the calibration curve was constructed via serial dilution of the same stock solution from which protein adsorption onto the hydrogels were studied and evaluated. In addition, the sensitivity of different methods of evaluation also varies. For example, as discussed, SDS-PAGE could not resolve the extremely low levels of other proteins absorbed. However, it does possess the advantages of simple operation and good reproducibility in the determination of protein molecular weight, detection of specific proteins, and identification of strain species,[26] and was applicable in this investigation for elucidating the pattern of the dominant adsorbed protein.

The impact of the complex nature of the proteins exposed to the implants *in vitro, ex vivo* and *in vivo* was evident. The protein adsorption potential of the hydrogels increased as the SBMA content increased in *ex vivo* fluids, however this variation was not significant ($p = 0.1046$ for AH and $p = 0.1047$ for VH). This observation is in opposition to that obtained from *in vitro* experiments with artificial protein solution in which the protein absorption decreased as the SBMA content increased. However, the protein absorption levels were significantly lower in both aqueous and vitreous humour *ex vivo* fluids vs the artificial protein solution ($p = 0.01284$ for AH and $p = 0.02286$ for VH). SBMA content contributed significantly to the variation in protein adsorption for the artificial protein solution ($p = 0.000531$). Thus, although the effect on SBMA content was evident both *in vitro* and *ex vivo*, its impact noted on exposure to an environment mimicking largely the anterior chamber ocular fluids is of most significance, with the protein composition of this ocular milieu corresponding more closely with the environment into which the hydrogel was implanted *in vivo* (subconjunctival).

Different studies have explored the proteomic fingerprint from the aqueous and vitreous humour. Stastna and colleagues found that the aqueous humour of rabbits contained approximately 400 µg of total protein (0.8 and 2.5 mg/mL when determined using the BCA assay).[27] The low level of adsorption observed may reflect the comparatively low level of total proteins found in the aqueous and vitreous humour of rabbits. The level of proteins in the aqueous and vitreous humours are also lower, and with a smaller variety of proteins, than that found in the tear fluid, hence the higher degree of protein absorption found in the *in vitro* artificial protein solution model.[28] In juvenile rabbits, however, Young and coworkers demonstrated procedure-dependent protein concentrations varying from 3.6 mg/mL in preoperative conditions to 12.1 mg/mL with IOL insertion hence, highlighting the capacity of an implantable device or biomaterial to stimulate protein release.[29] Even though their study was aimed at investigating the root causes of excessive scarring and immune response in children undergoing cataract

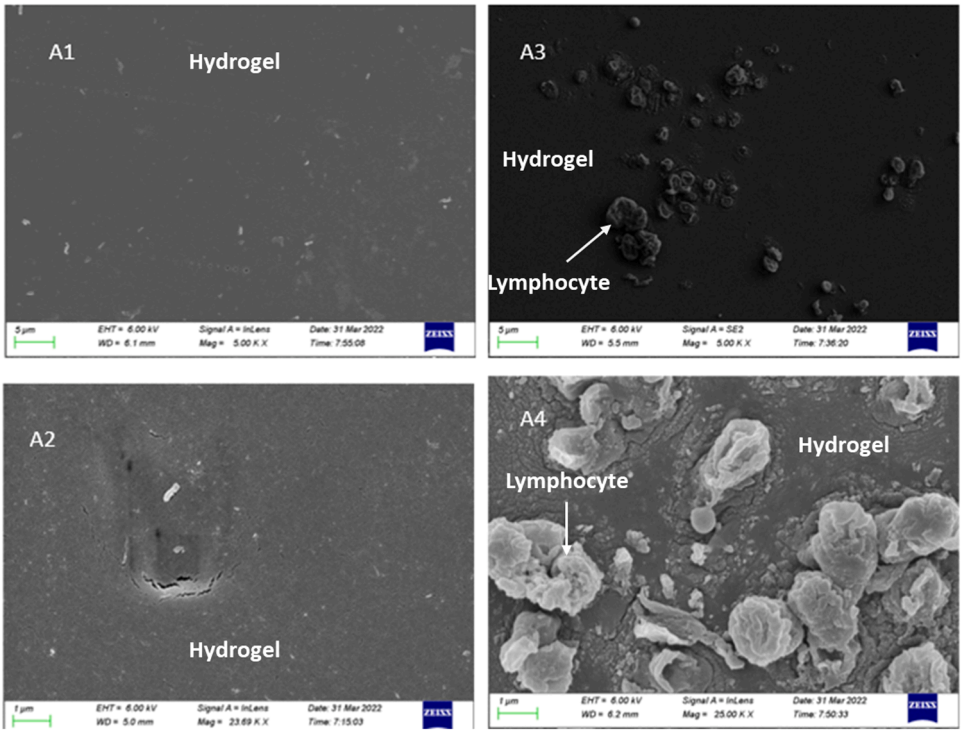

Fig. 12. SEM image of non-implanted controls of the hydrogel disc (A1 and A2) and the hydrogel disc explanted after 4 weeks (A3 and A4) at corresponding magnifications, showing lymphocytes.

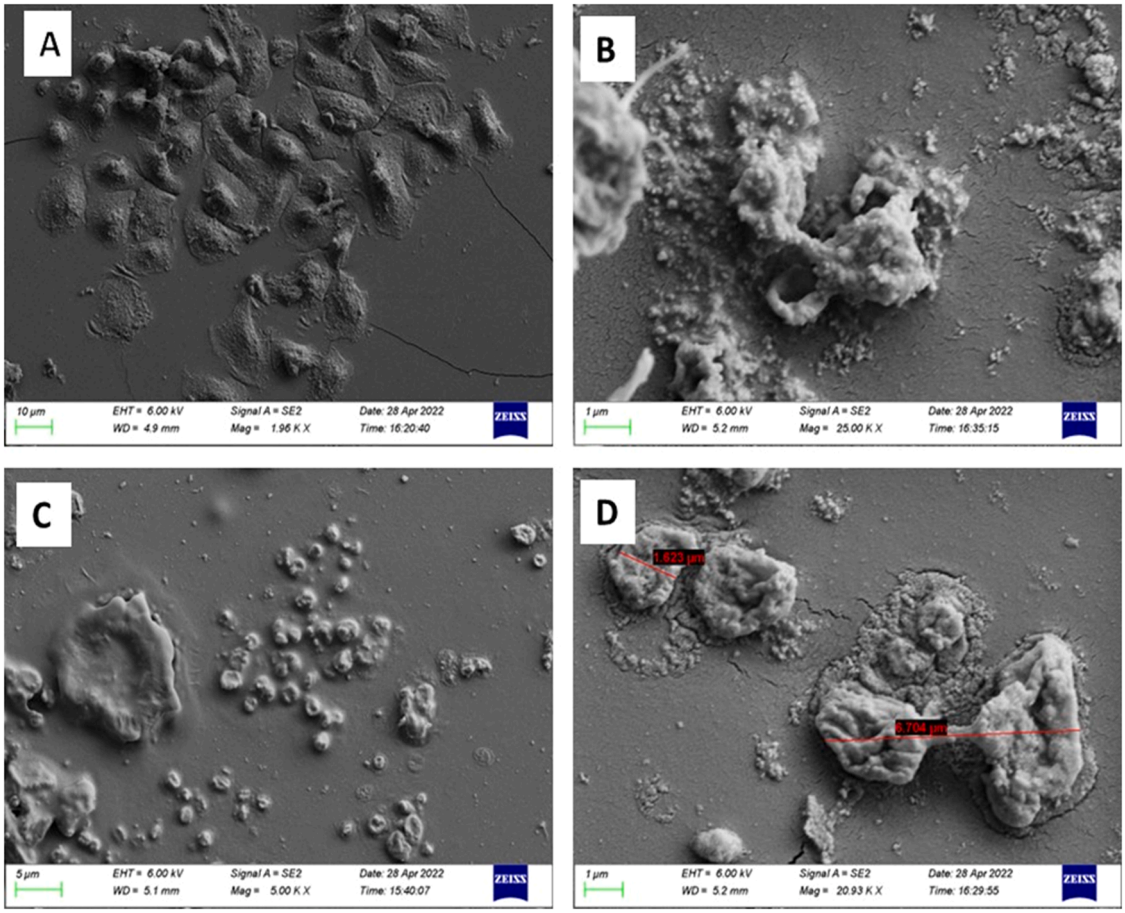

Fig. 13. SEM images of cells identified on representative hydrogels explanted after 8 weeks. Multinucleated giant body cell (A), Lymphocytes (B and D), and white blood cells (C).

surgery, the study relates the possible role that could be played by biomaterials in inducing protein influx that can act as cues for pro and anti-inflammatory macrophage polarization. It is pertinent to note that the total protein adsorbed by the hydrogels from an *in vitro* protein solution was higher than that adsorbed from the rabbit's ocular fluids as this suggests a greater propensity to limit protein adsorption under conditions of use. It is also important to note that the nature and type of proteins induced or attracted by a biomaterial depends to an extent on the properties of the biomaterial. Though there was a general reduction in the quantity of proteins adsorbed from ocular fluids, the somewhat reverse role played by the SBMA content of the hydrogel raises questions as to the nature of the interaction between the polymer and the proteins in the AH and VH ocular fluids particularly bearing in mind the unique nature of the ocular environment. Boone and colleagues also noted a difference in the quantity of lysozyme adsorbed from *ex vivo* tear fluid compared to *in vitro* measurements.[30] As with the current study, the total protein deposited in *in vitro* experiments were higher than that from *ex vivo* experiments, which they attributed to the complex nature of *ex vivo* protein creating the opportunity for competitive adsorption. In addition, the structural resemblance of SBMA to certain cell membrane proteins may contribute to this inverse relationship in terms of total proteins adsorbed as has been observed in this study. Zhang and colleagues previously demonstrated the stabilizing effect of polycarboxybetaine network within which the protein, uricase, was encapsulated,[31] to immunogenic attacks that usually result from repeated frequent protein injections. Contrary to these explanations, other investigations have indicated that protein-specific rather than formulation-specific factors are drivers of protein adsorption on nanoparticles in the vitreous.[32] There is therefore the need to explore this interaction and its applicability to different sites of insertion of the hydrogel within the ocular space with a view to harnessing the potential benefits from biomaterials modified by zwitterionic SBMA.

The proximity of ocular tissues often results in an orchestrated scarring in one tissue in response to effects on another tissue. The temporal cascade of events following biomaterial implantation is captured aptly by Maity and Sakar, [33] where they described the time modulated variation in acute, chronic and granulation tissue inflammation and the effect of cellular immune factors on intensity. The intensity and timeline of any of the phases depends on the degree of the injury inflicted, and the physicochemical properties of the biomaterial. Following surgical implantation of a biomaterial, an interplay between the biomaterial and the macrophage system (as the major markers of inflammatory/immune response) is initiated depending on the nature and types of protein that adheres on the biomaterial surface.[34]

Changes in the secondary structure of these adhering proteins will cause the macrophage system to either attack and phagocytize the biomaterial or to proceed with tissue repair (the so-called M1 and M2 polarization respectively). If the adhering proteins are identified as the same as membrane or body proteins, M2 macrophages are activated that initiate an anti-inflammatory response that tends towards tissue repair. To initiate tissue repair, M2 macrophages must be able to recognize and remove by-products of host protein oxidation that are generally termed danger associated molecular patterns (DAMP) and brought about by the action of reactive oxygen species released by the macrophages in the first instance.[35] Subsequently, these M2 macrophages serve as antigen presenting cells for the activation of T lymphocytes of the regulatory subset through the transforming growth factor β (TGF-β), platelet derived growth factor (PDGF), and interleukin 10 (IL-10) signalling.[35] T regulatory lymphocytes residing in non-lymphoid tissues perform a variety of functions in addition to their traditional immune suppressive roles specific to the context and their location.[36] In many biological procedures such as tissue engineering, surfaces that encourage protein adhesion and subsequent macrophage attachment are welcomed[6] whereas in other procedures, (in the eye particularly) such as implantation of IOL or in glaucoma drainage devices, macrophage adhesion following protein adsorption onto the device may lead to an extensive fibrotic response that ultimately deactivates the device and necessitates removal.[31,37] Understanding the nature of this interaction, therefore, becomes a prerequisite for designing biomaterials that could limit debilitating microenvironment pathologies.[38] The sensitive nature of the eye, which is the primary reason it operates an immune privilege environment, prohibits the inflammatory processes that often may lead to loss of sight. The conjunctiva is histologically differentiated into the epithelium and *substantia propria*. The *substantia propria,* composed of the adenoid and fibrous layer, is interspersed with a variety of tissues that together form the conjunctiva-associated lymphoid tissue (CALT) that modulates the immune and inflammatory responses around the ocular surface.[39,40] Inflammation was generally absent in most tissue specimens (confirmed by the general absence of multinucleated foreign body giant cells) and only minimally present in few sections (a multinucleated foreign body giant cell was noted in one section out of three sections in one sample) where it occurred and was related to the presence of hair shafts from the procedure. This observation agrees with the observations of Tan and colleagues that studied the uveal compatibility of MPC modified silicone hydrogel lenses.[41] The minimal presence of inflammatory components could derive from the fact that from the 4th to the 8th week all acute inflammatory response resulting from tissue injury would have subsided. Huang and co-workers (2016) prepared and evaluated a zwitterionic hydrogel reinforced with nanoclay as a wound dressing. They noted complete connective tissue formation and re-epithelization of the wound by the 12th day in diabetic rats.[42] In addition, removal of the dressing was clean without any adhering or intertwined tissues. Surface chemistry of biomaterials has been explored as a means of modulating inflammatory response to implanted devices. Surface wettability is one property that has frequently been exploited in this regard. Xu and colleagues investigated the adhesion of activated M1 and M2 macrophages onto hydrophobically modified methacrylated gellan gum and the subsequent expression of pro and anti inflammatory markers in RAW 264.7 cells culture media.[6] Their study confirmed that increasing hydrophobicity increased macrophage adhesion and reduced the expression of pro-inflammatory tumour necrosis factor-α (TNF-α). Shen and colleagues, on the other hand, studied the influence of the type of adsorbed protein on monocyte adhesion[36,43] and noted that adsorption of albumin reduced monocytes adhesion while fibronectin, plasma, serum, and immunoglobulin G adsorption promoted monocyte adhesion. Rostam and colleagues noted a different observation on the effect of hydrophobicity of biomaterial on the expression of pro-inflammatory markers.[37,44] Their study showed that increasing the hydrophilicity of polystyrene via plasma O_2 etching caused the polarization of macrophages toward the M1 pro-inflammatory end. Even though there are conflicting reports on the influence of surface wettability on the macrophage phenotype polarization, it is clear that the type and conformation of adsorbed protein on a surface determines the polarization of macrophages since macrophages will adhere to any surface in their natural line of action, irrespective of the surface wettability, particularly in the presence of tissue injury during implantation. In addition, other biomaterial properties such as topography and stiffness contribute to protein adhesion and invariably to macrophage adhesion and polarization. Ultimately, the importance of *in vivo* confirmatory studies is further brought to the fore. What is of overriding importance is the need to design biomaterial surfaces that polarize macrophages towards the specific requirements of the particular application intended. The *in vivo* study undertaken here has shown that the observed macrophage adhesion onto the implant caused a macrophage polarization towards an anti-inflammatory effect, given the absence of inflammation after one week. These outcomes represent an advancement compared to the characteristics of many existing biomaterials utilized in ocular devices such as contact lenses (that are employed in the treatment and diagnosis of ocular diseases) with respect to their interaction with body fluid - an interaction on which their success depends.

Often, implanted biomaterials act as a consistent and continuous inflammatory stimulus that eventually results in a cytokine storm when

inflammatory cells are not able to cordon off the biomaterial. The capsule formation effectively cordons off the biomaterial device from the biological environment and in applications used as sensors, this effectively leads to device failure as the device will lose connection with the stimulus. If, however, the fibrotic capsule is perfused with connective tissue, the contact with the biological environment is maintained alongside the functions of such devices. The acute inflammatory response to a normal wound that is targeted at tissue repair generally begins to resolve by the third week after surgery [3404] and this is evident in the histological observations obtained at 4 weeks.

The disappearance of some implanted hydrogel discs indicates the requirement to study the extrusion potential and rate from the conjunctiva should the developed implant be planned for as an implantable drug delivery device for further preclinical and clinical assessment.

Conclusion

This work has demonstrated the potential of the novel biomaterial developed and evaluated herein to limit inflammation in a New Zealand albino rabbit eye model, highlighting its potential as an ocular delivery device. Zwitterionisation with SBMA significantly influenced the anti-inflammatory tissue repair process. Investigations demonstrated that protein adsorption studies *in vitro* from complex protein solutions do not always reflect that from *ex vivo* biological fluids, particularly with regards to the ocular environment. It could also highlight that zwitterionisation with SBMA may serve a more significant antifouling role for ocular implants introduced to the anterior chamber of the anterior segment of the eye versus implants targeted for posterior insertion. Likewise, zwitterionization was instrumental in ensuring that the anti-inflammatory response to the hydrogels implanted subconjunctivally in rabbit's eye tended towards the natural repair process. Future research would explore the drug delivery potential of the hydrogel when utilized in the fabrication of devices such as contact lenses that would serve the dual function of vision correction and delivery, with potential exploration in human models (e.g. human corneal models still under development[45]).

Funding

This work was supported by the National Research Foundation (NRF) of South Africa [grant number: 64814].

Data availability statement

All data generated or analysed during the current study are available from the corresponding author on reasonable request.

Declaration of competing interest

The authors declare that they have no known competing financial interests or personal relationships that could have appeared to influence the work reported in this paper.

References

1. Uwaezuoke OJ, Kumar P, Pillay V, Choonara YE. Fouling in ocular devices: implications for drug delivery, bioactive surface immobilization, and biomaterial design. *Drug Deliv Transl Res*. 2021. https://doi.org/10.1007/s13346-020-00879-1. Published online January 16.
2. Inomata T, Sung J. Changing medical paradigm on inflammatory eye disease: technology and its implications for P4 medicine. *J Clin Med*. 2022;11(11):2964. https://doi.org/10.3390/jcm11112964.
3. Punctal Plugs. American Academy of Ophthalmology. 2023. Accessed May 26, 2023. https://www.aao.org/eye-health/diseases/punctal-plugs.
4. 12 Devices for Treating Dry Eyes. American Academy of Ophthalmology. 2020. Accessed May 26, 2023. https://www.aao.org/eye-health/tips-prevention/how-to-treat-dry-eye-devices.
5. Lužajić Božinovski T, Todorović V, Milošević I, et al. Macrophages, the main marker in biocompatibility evaluation of new hydrogels after subcutaneous implantation in rats. *J Biomater Appl*. 2022;36(6):1111–1125. https://doi.org/10.1177/08853282211046119.
6. Xu Z, Hwang DG, Bartlett MD, Jiang S, Bratlie KM. Alter macrophage adhesion and modulate their response on hydrophobically modified hydrogels. *Biochem Eng J*. 2021;165, 107821. https://doi.org/10.1016/j.bej.2020.107821.
7. Ishihara K, Fukazawa K, Sharma V, et al. Antifouling silicone hydrogel contact lenses with a bioinspired 2-methacryloyloxyethyl phosphorylcholine polymer surface. *ACS Omega*. 2021;6(10):7058–7067. https://doi.org/10.1021/acsomega.0c06327.
8. Jansen LE, Amer LD, Chen EYT, et al. Zwitterionic PEG-PC hydrogels modulate the foreign body response in a modulus-dependent manner. *Biomacromolecules*. 2018;19(7):2880–2888. https://doi.org/10.1021/acs.biomac.8b00444.
9. Lynch CR, Kondiah PPD, Choonara YE, du Toit LC, Ally N, Pillay V. Hydrogel biomaterials for application in ocular drug delivery. *Front Bioeng Biotechnol*. 2020;8. Accessed March 17, 2022 https://www.frontiersin.org/article/10.3389/fbioe.2020.00228.
10. Vigata M, Meinert C, Hutmacher DW, Bock N. Hydrogels as drug delivery systems: a review of current characterization and evaluation techniques. *Pharmaceutics*. 2020;12(12):1188. https://doi.org/10.3390/pharmaceutics12121188.
11. Uwaezuoke OJ, Kumar P, du Toit L, Ally N, Choonara Y. *The design characteristics of a neoteric, superhydrophilic, mechanically robust hydrogel engineered to limit fouling in the ocular environment. ACS Omega*. June 2024. Published online.
12. Synthesis of polyvinyl alcohol with methacrylate groups and of hydrogels based on it | SpringerLink. Accessed September 24, 2021. https://link.springer.com/article/10.1134/S1070427215040102.
13. Xiang T, Lu T, Xie Y, Zhao WF, Sun SD, Zhao CS. Zwitterionic polymer functionalization of polysulfone membrane with improved antifouling property and blood compatibility by combination of ATRP and click chemistry. *Acta Biomater*. 2016;40:162–171. https://doi.org/10.1016/j.actbio.2016.03.044.
14. Boychev N, Yeung V, Yang M, Kanu LN, Ross AE, Kuang L, Chen L, Ciolino JB. Ocular tear fluid biomarkers collected by contact lenses. *Biochem Biophys Res Comm*. 2024;734, 150744. https://doi.org/10.1016/j.bbrc.2024.150744.
15. Zhang W, Li G, Lin Y, Wang L, Wu S. Preparation and characterization of protein-resistant hydrogels for soft contact lens applications via radical copolymerization involving a zwitterionic sulfobetaine comonomer. *J Biomater Sci Polym Ed*. 2017;28(16):1935–1949. https://doi.org/10.1080/09205063.2017.1363127.
16. Stastna M, Behrens A, Noguera G, Herretes S, McDonnell P, Van Eyk JE. Proteomics of the aqueous humor in healthy New Zealand rabbits. *Proteomics*. 2007;7:4358–4375. https://doi.org/10.1002/pmic.200700300.
17. Mandal N, Lewis GP, Fisher SK, Heegaard S, Prause JU, la Cour M, Vorum H, Honoré B. Proteomic analysis of the vitreous following experimental retinal detachment in rabbits. *J Ophthalmol*. 2015;2015, 583040. https://doi.org/10.1155/2015/583040.
18. Zhang Z, Chao T, Liu L, Cheng G, Ratner BD, Jiang S. Zwitterionic hydrogels: an in vivo implantation study. *J Biomater Sci Polym Ed*. 2009;20(13):1845–1859. https://doi.org/10.1163/156856208×386444.
19. Acosta AC, Espana EM, Yamamoto H, et al. A newly designed glaucoma drainage implant made of Poly(styrene-b-isobutylene-b-styrene): biocompatibility and function in normal rabbit eyes. *Arch Ophthalmol*. 2006;124(12):1742–1749. https://doi.org/10.1001/archopht.124.12.1742.
20. Wang J, Liu X, Zhang Y, Liu F, Zhu J. Modification of poly(ethylene 2,5-furandicarboxylate) with 1,4-cyclohexanedimethylene: influence of composition on mechanical and barrier properties. *Polymer*. 2016;103:1–8. https://doi.org/10.1016/j.polymer.2016.09.030.
21. Ramsay E, del Amo EM, Toropainen E, et al. Corneal and conjunctival drug permeability: systematic comparison and pharmacokinetic impact in the eye. *Eur J Pharm Sci*. 2018;119:83–89. https://doi.org/10.1016/j.ejps.2018.03.034.
22. Ashtiani MK, Zandi M, Shokrollahi P, Ehsani M, Baharvand H. Surface modification of poly(2-hydroxyethyl methacrylate) hydrogel for contact lens application. *Polym Adv Technol*. 2018;29(4):1227–1233. https://doi.org/10.1002/pat.4233.
23. Goda T, Matsuno R, Konno T, Takai M, Ishihara K. Protein adsorption resistance and oxygen permeability of chemically crosslinked phospholipid polymer hydrogel for ophthalmologic biomaterials. *J Biomed Mater Res B Appl Biomater*. 2009;89(1):184–190. https://doi.org/10.1002/jbm.b.31204.
24. Phan CM, Bajgrowicz-Cieslak M, Subbaraman LN, Jones L. Release of moxifloxacin from contact lenses using an in vitro eye model: impact of artificial tear fluid composition and mechanical rubbing. *Transl Vis Sci Technol*. 2016;5(6):3. https://doi.org/10.1167/tvst.5.6.3.
25. Skeie JM, Roybal CN, Mahajan VB. Proteomic insight into the molecular function of the vitreous. *PLoS One*. 2015;10(5), e0127567. https://doi.org/10.1371/journal.pone.0127567.
26. Tantray JA, Mansoor S, Choh Wani RF, Un Nissa N. *Chapter 21 - To identify a protein sample using SDS-PAGE. Basic Life Science Methods. A Laboratory Manual for Students and Researchers*. 2023:87–92.
27. Stastna M, Behrens A, McDonnell PJ, Van Eyk JE. Analysis of protein composition of rabbit aqueous humor following two different cataract surgery incision procedures using 2-DE and LC-MS/MS. *Proteome Sci*. 2011;9:8. https://doi.org/10.1186/1477-5956-9-8.
28. Beisel A, Jones G, Glass J, Jin Lee T, Töteberg-Harms M, Estes A, Ulrich L, Bollinger K, Sharma S, Sharma A. Comparative analysis of human tear fluid and aqueous humor proteomes. *Ocular Surf*. 2024;33:16–22.
29. Young JB, Keppel TR, Waas M, et al. Quantitative proteomic analysis of aqueous humor after rabbit lensectomy reveals differences in coagulation and immunomodulatory proteins. *Mol Omics*. 2020;16(2):126–137. https://doi.org/10.1039/C9MO00169G.

30. Boone A, Heynen M, Joyce E, Varikooty J, Jones L. Ex vivo protein deposition on bi-weekly silicone hydrogel contact lenses. *Optom Vis Sci*. 2009;86(11):1241–1249. https://doi.org/10.1097/OPX.0b013e3181bbc1b3.
31. Zhang P, Sun F, Tsao C, et al. Zwitterionic gel encapsulation promotes protein stability, enhances pharmacokinetics, and reduces immunogenicity. *Proc Natl Acad Sci*. 2015;112(39):12046–12051. https://doi.org/10.1073/pnas.1512465112.
32. Tavakoli S, Kalevi Kari O, Turunen T, Lajunen T, Schmitt M, Lehtinen J, Tasaka F, Parkkila P, Ndika J, Viitala T, Alenius H, Urtti A, Subrizi A. Diffusion and protein corona formation of lipid-based nanoparticles in the vitreous humor: profiling and pharmacokinetic considerations. *Mol. Pharm*. 2021;18(2):699–713. https://doi.org/10.1021/acs.molpharmaceut.0c00411.
33. Maity S, Sarkar A. 4 - Monitoring fibrous capsule formation. In: Narayan RJ, ed. *Monitoring and Evaluation of Biomaterials and Their Performance In Vivo*. Woodhead Publishing; 2017:69-80. doi:10.1016/B978-0-08-100603-0.00004-3.
34. Gordon S, Plüddemann A. Tissue macrophages: heterogeneity and functions. *BMC Biol*. 2017;15(1):53. https://doi.org/10.1186/s12915-017-0392-4.
35. Hilhorst M, Shirai T, Berry G, Goronzy JJ, Weyand CM. T cell–macrophage interactions and granuloma formation in vasculitis. *Front Immunol*. 2014;5. Accessed May 14, 2022 https://www.frontiersin.org/article/10.3389/fimmu.2014.00432.
36. Traxinger BR, Richert-Spuhler LE, Lund JM. Mucosal tissue regulatory T cells are integral in balancing immunity and tolerance at portals of antigen entry. *Mucosal Immunol*. 2022;15(3):398–407. https://doi.org/10.1038/s41385-021-00471-x.
37. Mahale A, Othman MW, Shahwan SA, et al. Altered expression of fibrosis genes in capsules of failed Ahmed glaucoma valve implants. *PLoS One*. 2015;10(4), e0122409. https://doi.org/10.1371/journal.pone.0122409.
38. Vishwakarma A, Bhise NS, Evangelista MB, et al. Engineering immunomodulatory biomaterials to tune the inflammatory response. *Trends Biotechnol*. 2016;34(6):470–482. https://doi.org/10.1016/j.tibtech.2016.03.009.
39. Arnous R, Arshad S, Sandgren K, Cunningham AL, Carnt N, White A. Tissue resident memory T cells inhabit the deep human conjunctiva. *Sci Rep*. 2022;12(1):6077. https://doi.org/10.1038/s41598-022-09886-3.
40. Rohner NA, Learn GD, Wiggins MJ, Woofter RT, von Recum HA. Characterization of inflammatory and fibrotic encapsulation responses of implanted materials with bacterial infection. *ACS Biomater Sci Eng*. 2021;7(9):4474–4482. https://doi.org/10.1021/acsbiomaterials.1c00505.
41. Tan X, Zhan J, Zhu Y, et al. Improvement of uveal and capsular biocompatibility of hydrophobic acrylic intraocular lens by surface grafting with 2-methacryloyloxyethyl phosphorylcholine-methacrylic acid copolymer. *Sci Rep*. 2017;7, 40462. https://doi.org/10.1038/srep40462.
42. Huang KT, Fang YL, Hsieh PS, Li CC, Dai NT, Huang CJ. Zwitterionic nanocomposite hydrogels as effective wound dressings. *J Mater Chem B*. 2016;4(23):4206–4215. https://doi.org/10.1039/C6TB00302H.
43. Shen M, Horbett TA. The effects of surface chemistry and adsorbed proteins on monocyte/macrophage adhesion to chemically modified polystyrene surfaces. *J Biomed Mater Res*. 2001;57(3):336–345. https://doi.org/10.1002/1097-4636(20011205)57:3<336::aid-jbm1176>3.0.co;2-e.
44. Rostam HM, Singh S, Salazar F, et al. The impact of surface chemistry modification on macrophage polarisation. *Immunobiology*. 2016;221(11):1237–1246. https://doi.org/10.1016/j.imbio.2016.06.010.
45. Shiju TM, Carlos de Oliveira R, Wilson SE. 3D in vitro corneal models: a review of current technologies. *Exp Eye Res*. 2020;200, 108213. https://doi.org/10.1016/j.exer.2020.108213.